

1 **Role of endogenous adenine in kidney failure and mortality with diabetes**

2
3 Kumar Sharma, M.D.^{1,2*}, Guanshi Zhang, Ph.D.^{1,2}, Jens Hansen, M.D.³, Petter Bjornstad, M.D.⁴, Hak Joo Lee,
4 Ph.D.^{1,2}, Rajasree Menon, Ph.D.⁵, Leila Hejazi, Ph.D.^{1,6}, Jian-Jun Liu, MBBS⁷, Anthony Franzone, B.S.¹, Helen C.
5 Looker, MBBS⁸, Byeong Yeob Choi, Ph.D.^{1,9}, Roman Fernandez, M.S.⁹, Manjeri A. Venkatachalam, MBBS^{1,10},
6 Luxcia Kugathasan, BSc¹¹, Vikas S. Sridhar, M.D.¹¹, Loki Natarajan, Ph.D.¹², Jing Zhang, M.S.¹², Varun Sharma,
7 M.Sc.¹³, Brian Kwan, Ph.D.¹⁴, Sushrut Waikar, M.D.¹⁵, Jonathan Himmelfarb, M.D.¹⁶, Katherine Tuttle, M.D.¹⁶, Bryan
8 Kestenbaum, M.D.¹⁶, Tobias Fuhrer, Ph.D.¹⁷, Harold Feldman, M.D.¹⁸, Ian H. de Boer, M.D.¹⁶, Fabio C. Tucci,
9 Ph.D.¹⁹, John Sedor, M.D.²⁰, Hiddo Lambers Heerspink, Ph.D.^{21,22}, Jennifer Schaub, M.D.⁵, Edgar Otto, Ph.D.⁵,
10 Jeffrey B. Hodgin, M.D.⁵, Matthias Kretzler, M.D.⁵, Christopher Anderton, Ph.D.^{1,23}, Theodore Alexandrov, Ph.D.²⁴,
11 David Cherney, M.D.¹¹, Su Chi Lim, MBBS^{7,25,26,27}, Robert G. Nelson M.D.⁸, Jonathan Gelfond, M.D.^{1,9}, Ravi Iyengar,
12 Ph.D.³; for the Kidney Precision Medicine Project

- 13 1. Center for Precision Medicine, The University of Texas Health San Antonio, TX
- 14 2. Division of Nephrology, Department of Medicine, The University of Texas Health San Antonio, TX, USA
- 15 3. Department of Pharmacological Sciences and Institute for Systems Biomedicine, Icahn School of Medicine
16 at Mount Sinai, New York, NY, USA
- 17 4. Division of Nephrology, Department of Medicine and Section of Endocrinology, Department of Pediatrics,
18 University of Colorado Anschutz Medical Campus, Aurora, CO, USA
- 19 5. Department of Internal Medicine, University of Michigan, Ann Arbor, Michigan, USA
- 20 6. SygnaMap, Inc., San Antonio, TX
- 21 7. Clinical Research Unit, Khoo Teck Puat Hospital, Singapore
- 22 8. Chronic Kidney Disease Section, National Institute of Diabetes and Digestive and Kidney Diseases, Phoenix,
23 AZ
- 24 9. Department of Population Health Sciences, University of Texas Health San Antonio, 7703 Floyd Curl Drive,
25 San Antonio, TX, 78229, USA
- 26 10. Department of Pathology, University of Texas Health San Antonio, TX, USA

- 27 11. Department of Medicine, Division of Nephrology, University Health Network, Toronto, Ontario, Canada.
28 Department of Physiology, University of Toronto, Toronto, Ontario, Canada; Cardiovascular Sciences
29 Collaborative Specialization, University of Toronto, Toronto, Canada
- 30 12. Department of Family Medicine and Public Health, Herbert Wertheim School of Public Health, University of
31 California-San Diego, La Jolla, California. University of California-San Diego Moores Cancer Center,
32 University of California-San Diego, La Jolla, California
- 33 13. Center for Molecular Medicine, Vienna, Austria
- 34 14. Department of Biostatistics, Fielding School of Public Health, University of California, Los Angeles,
35 California
- 36 15. Division of Nephrology, Department of Medicine, Boston University, Boston, MA
- 37 16. Department of Medicine, University of Washington, Seattle, WA, USA, Division of Nephrology, Department
38 of Medicine, Kidney Research Institute, University of Washington, Seattle, Washington, USA
- 39 17. Institute of Molecular Systems Biology, ETH Zurich, 8093, Zurich, Switzerland
- 40 18. Center for Clinical Epidemiology and Biostatistics, Perelman School of Medicine at the University of
41 Pennsylvania, Department of Biostatistics, Epidemiology, and Informatics, Perelman School of Medicine at
42 the University of Pennsylvania
- 43 19. Epigen Biosciences, Inc., San Diego, California, USA
- 44 20. Cleveland Clinic, Cleveland, Ohio
- 45 21. Department of Clinical Pharmacy and Pharmacology, University Medical Center Groningen, Groningen, the
46 Netherlands
- 47 22. The George Institute for Global Health, Sydney, Australia
- 48 23. Environmental Molecular Sciences Laboratory, Pacific Northwest National Laboratory, Richland, WA, USA
- 49 24. Structural and Computational Biology Unit, European Molecular Biology Laboratory, Heidelberg, Germany
- 50 25. Diabetes Center, Admiralty Medical Center, Khoo Teck Puat Hospital, Singapore
- 51 26. Saw Swee Hock School of Public Health, National University of Singapore, Singapore
- 52 27. Lee Kong Chian School of Medicine, Nanyang Technological University, Singapore

53

54 *Corresponding Author: Kumar Sharma, MD (Email: sharmak3@uthscsa.edu; Tel: 210-567-4700)

55 **Abstract**

56 Diabetic kidney disease (DKD) can lead to end-stage kidney disease (ESKD) and mortality, however, few mechanistic
57 biomarkers are available for high risk patients, especially those without macroalbuminuria. Urine from participants
58 with diabetes from Chronic Renal Insufficiency Cohort (CRIC), Singapore Study of Macro-Angiopathy and Reactivity
59 in Type 2 Diabetes (SMART2D), and the Pima Indian Study determined if urine adenine/creatinine ratio (UAdCR)
60 could be a mechanistic biomarker for ESKD. ESKD and mortality were associated with the highest UAdCR tertile in
61 CRIC (HR 1.57, 1.18, 2.10) and SMART2D (HR 1.77, 1.00, 3.12). ESKD was associated with the highest UAdCR
62 tertile in patients without macroalbuminuria in CRIC (HR 2.36, 1.26, 4.39), SMART2D (HR 2.39, 1.08, 5.29), and
63 Pima Indian study (HR 4.57, CI 1.37-13.34). Empagliflozin lowered UAdCR in non-macroalbuminuric participants.
64 Spatial metabolomics localized adenine to kidney pathology and transcriptomics identified ribonucleoprotein
65 biogenesis as a top pathway in proximal tubules of patients without macroalbuminuria, implicating mammalian target
66 of rapamycin (mTOR). Adenine stimulated matrix in tubular cells via mTOR and stimulated mTOR in mouse kidneys.
67 A specific inhibitor of adenine production was found to reduce kidney hypertrophy and kidney injury in diabetic mice.
68 We propose that endogenous adenine may be a causative factor in DKD.

69

70 **Introduction**

71 Progression to organ failure is marked by fibrosis and loss of architecture in solid organs, such as the kidney. In almost
72 all progressive chronic kidney diseases (CKD) the features that are most consistently associated with functional loss
73 of the glomerular filtration rate (GFR) are the degree of glomerulosclerosis, tubulointerstitial fibrosis, vascular injury,
74 and proteinuria (1-4). However, many patients who eventually develop end-stage kidney disease (ESKD) are non-
75 proteinuric at the time impaired GFR is recognized. Non-proteinuria is defined as urine albumin-to-creatinine ratio
76 (ACR) ≤ 300 mg/creatinine or urine albumin excretion ≤ 300 mg/day (5). As non-proteinuric or non-macroalbuminuric
77 DKD accounts for >40% of prevalent ESKD in patients with type 2 diabetes (5-7) and 75% of prevalent CKD (GFR
78 <60 mL/min/1.73m²) (8) identifying the patients at risk for progression in early stages of disease is an important step
79 to improve clinical outcomes. This is especially relevant as the armamentarium of therapies for DKD to mitigate
80 kidney disease progression has rapidly expanded (9-11).

81 Establishing novel biomarkers that predict progression and represent biologically relevant pathways in DKD
82 could improve the care of patients with diabetes. To identify novel biomarkers, we recently performed an untargeted

83 urine metabolomics study in patients with type 2 diabetes (T2D) and impaired eGFR from the Chronic Renal
84 Insufficiency Cohort (CRIC) study (12) and identified 15 candidate metabolites associated with ESKD. A targeted
85 assay validated 13 of these metabolites, one of which was adenine. As exogenous adenine has been found to cause
86 kidney failure in mice, rats, and dogs (13-15), we evaluated whether endogenous adenine could play a role in
87 progression of kidney disease in patients with diabetes.

88

89 **Results**

90 *Urine adenine/creatinine ratio predicts kidney failure and all cause mortality in the CRIC and SMART2D cohorts.*

91 The baseline clinical characteristics of the participants with diabetes from CRIC and SMART2D are shown in Table
92 1. Of the 904 subjects evaluated from CRIC, 558 had either normoalbuminuria or microalbuminuria, 341 had
93 macroalbuminuria, and 5 had no data for 24h albumin. The mean eGFR was 40 mL/min/1.73m². The top tertile of
94 baseline urine adenine/creatinine ratio (UAdCR) was found to identify the participants with diabetes who were at high
95 risk for ESKD and all cause mortality (adjusted HR 1.57, 95% CI 1.18, 2.10, as compared to the lowest tertile) (Figure
96 1A) and a similar significant relationship was found using UAdCR as a continuous variable (Table 2). The value of
97 the top tertile of UAdCR to identify patients with diabetes at high risk for ESKD and all cause mortality was confirmed
98 in participants from SMART2D who had reduced eGFR and normoalbuminuria or microalbuminuria (adjusted HR
99 1.77, 95% CI 1.00, 3.12) (Figure 1B, Table 2, datasets combined in Supplementary Figure 2A).

100 *UAdCR predicts kidney failure in the non-macroalbuminuric Pima, CRIC, and SMART2D cohorts and*
101 *empagliflozin reduces UAdCR.* The UAdCR was also evaluated in early-stage disease (measured GFR>90
102 mL/min/1.73m²) in a Pima Indian cohort with >20 year follow up (Table 1). As the majority of the participants in the
103 Pima Indian cohort had non-macroalbuminuria (n=42 of the 54 participants), the association of UAdCR with
104 longitudinal progression to ESKD is presented in this non-macroalbuminuric cohort. ESKD was associated with the
105 top UAdCR tertile (HR 4.57, CI 1.37-13.34) (Supplementary Table 1). UAdCR was also measured from 2 untimed
106 spot urine samples obtained 1 year apart and found to be consistent across the individual paired samples (r=0.665,
107 p<0.0001) (Supplementary Figure 3). Similar relationships to predict ESKD was found in the non-macroalbuminuric
108 participants in CRIC (adjusted HR 2.36, 95% CI 1.26, 4.39) and SMART2D (adjusted HR 2.39, 95% CI 1.08, 5.29)
109 (Figure 2A, 2B, Supplementary Table 2, combined datasets in Supplementary Figure 2B). Of note, there were no
110 significant correlations of UAdCR with the UACR or eGFR in the non-macroalbuminuric subjects from CRIC or

111 SMART2D (Supplementary Table 3). Of the CRIC subjects with macroalbuminuria, there were modest associations
112 between the top tertile of UAdCR and ESKD (HR 1.10, CI 0.75, 1.60) and mortality (HR 1.33, CI 0.59, 3.01).

113 To determine if UAdCR could be modified in non-macroalbuminuric participants with normal or elevated
114 measured GFR by glycemia or a therapeutic intervention with an SGLT2 inhibitor, the UAdCR was measured during
115 euglycemia or hyperglycemia before and after empagliflozin in patients with T1D (clinical characteristics described
116 in Supplementary Table 4). Acute hyperglycemia did not alter UAdCR levels (Supplementary Figure 4), however
117 empagliflozin significantly lowered UAdCR by 36.4% (Figure 2C).

118 *Adenine is localized to regions of kidney fibrosis and is increased in patients with diabetes.* A spatial
119 metabolomics platform was developed to annotate small molecules (<700 Da) and performed on kidney biopsies from
120 healthy controls and in patients with diabetes (clinical characteristics in Supplementary Table 4). Adenine was present
121 at low intensity in normal glomeruli and blood vessels in the healthy control kidney (Figure 3A) and enhanced in
122 regions of arteriolosclerosis, tubulointerstitial fibrosis and early glomerulosclerosis in the diabetic kidney (Figure 3B).
123 There was an overall increase in adenine in the whole section of kidney biopsies from participants with diabetes as
124 compared to healthy controls (Figure 3C). The spatial adenine values in rat kidney sections were found to correlate
125 well with the UAdCR in a ZDF diabetic model ($r=0.73$, $p<0.001$, Supplementary Table 5).

126 *Single cell transcriptomics identify ribonucleoprotein biogenesis as a dominant pathway in non-*
127 *macroalbuminuric DKD.* As adenine was prominent in regions of tubular pathology in the diabetic kidney and
128 empagliflozin treatment lowered the UAdCR in patients, the proximal tubular cells were considered to be a target cell
129 type affected by adenine. Single cell transcriptomics from proximal tubular cells were studied in DKD patients from
130 the KPMP study ($n=28$) and an unbiased pathway analysis was performed based on differentially regulated genes. The
131 top pathway identified was the ribosomal nucleoprotein biogenesis pathway in patients without macroalbuminuria and
132 low eGFR (Figure 4A, B). In addition, small and large ribosomal subunit organization pathways were also upregulated
133 in these patients. Replication of these results from KPMP was found in the CROCODILE study in diabetic patients
134 without macroalbuminuria and normal GFR (Figure 4C). As ribonucleoprotein biogenesis, and small and large
135 ribosomal subunit organization is closely linked to activity of mammalian target of rapamycin (mTOR) (16) and
136 adenine has been found to stimulate mTOR (17), this pathway was evaluated to mediate adenine-induced effects on
137 proximal tubular cells.

138 *Mechanism of adenine induced matrix production is via the mTOR pathway and adenine increases KIM1 and*
139 *sTNFR1 in mice.* To determine whether adenine could be in the causative pathway for tissue fibrosis, adenine was
140 added to mouse and human proximal tubular cells. There was a robust and early stimulation of fibronectin by adenine
141 (Figure 4D, Supplementary Figure 5A). In addition, adenine stimulated mTOR activity as demonstrated by enhanced
142 phosphorylation of S6 kinase (Figure 4E, Supplementary Figure 5B). Inhibition of mTORC1 with rapamycin blocked
143 adenine-induced production of fibronectin (Figure 4E, 4F). Exposure of adenine to normal mice stimulated blood and
144 kidney levels of soluble tumor necrosis factor receptor 1 (sTNFR1) and kidney injury molecule-1 (KIM1), kidney
145 hypertrophy, kidney mTOR activity, and kidney matrix production (Figures 4 G-K; Supplementary Figure 6).

146 *Endogenous adenine contributes to diabetic kidney disease in db/db mice.* To determine whether endogenous
147 adenine plays a role in progression of diabetic kidney disease, methylthio-DADMe-Immucillin-A (MTDIA) a small
148 molecule specific inhibitor of methylthioadenosine phosphorylase (MTAP) was administered to db/db mice, a model
149 of obese type 2 diabetes. MTAP converts methylthioadenosine to adenine and is responsible for approximately 80%
150 of adenine production in mammalian cells (18). MTDIA was well tolerated and did not affect food intake, water intake,
151 blood glucose levels or body weight (Supplementary Table 6). MTDIA significantly reduced kidney adenine in db/db
152 mice (Figure 5A) but not other metabolites linked to progression of kidney disease (Supplementary Table 7) (19).
153 MTDIA significantly reduced serum cystatin C, kidney hypertrophy, kidney KIM1, and partially reduced urine ACR,
154 serum creatinine, urine KIM1, kidney matrix proteins and mTOR activity in db/db mice (Figure 5 B-I).

155

156 **Discussion**

157 The results from the present study demonstrate a role for endogenous adenine in kidney disease progression in the
158 context of DKD. Urine levels of the AdCR identified patients with diabetes at high risk of kidney failure and all cause
159 mortality at all levels of albuminuria in the CRIC study and verified in a cohort study from Singapore. The UAdCR
160 can also identify patients who will develop ESKD even in the setting of normal or elevated GFR without
161 macroalbuminuria across ethnicities. Spatial metabolomics localized adenine to regions of vascular, tubular, and
162 glomerular pathology in patients with diabetes who have normoalbuminuria and GFR. Adenine appears to be in the
163 causal pathway of kidney fibrosis as adenine was demonstrated to stimulate matrix molecules in proximal tubular cells
164 via mTOR, was causative of kidney matrix production in mice and inhibiting adenine production was protective in
165 diabetic mice.

166 Biomarkers in the causal pathway have not previously been identified for kidney disease progression in non-
167 macroalbuminuric patients with diabetes. Microalbuminuria is clearly a risk factor for kidney disease progression,
168 however as microalbuminuria can revert to normoalbuminuria (20) the dependence upon microalbuminuria alone may
169 not provide reliable prognostication for event rates of GFR decline or kidney failure. Non-invasive omics approaches
170 using plasma and urine have identified promising candidate biomarkers (21-23), however, demonstration of a
171 contributory role of these biomarkers to the disease process has been difficult to establish (24). In the present study,
172 integration of spatial metabolomics and single cell transcriptomics of human kidney biopsies converged on adenine
173 and the mTOR pathway as highly relevant to DKD progression. The link with adenine and pathologic features was
174 suggested by spatial metabolomics as adenine could be localized adjacent to atrophic tubules, in regions of
175 arteriosclerotic blood vessels and glomerulosclerosis. The spatial localization implicated adenine to potentially be an
176 endogenous pro-fibrotic factor.

177 Adenine is known to cause kidney pathology as an exogenous toxin in mouse (25) and rat models (14) of CKD,
178 and possibly as an endogenous toxin in humans (26). The pathology of adenine-induced kidney disease includes
179 glomerulosclerosis, tubular atrophy, interstitial fibrosis, and inflammatory cell infiltration (27, 28). The mechanism
180 of adenine induced kidney disease has not been established although it has been postulated that conversion of adenine
181 to 2-8 dihydroxyadenine (26) is a driver of CKD in patients with mutations of adenine phosphoribosyltransferase
182 (APRT), the major enzyme that metabolizes adenine to AMP. However, CKD patients with APRT mutations are rare.
183 Adenine itself is likely an endogenous tubular toxin based on the spatial metabolomic analysis and our finding that
184 high urine adenine identifies patients at high risk of ESKD. Adenine exposure enhances tubular cell matrix production
185 via the mTOR pathway and a prior study found that adenine is a potent stimulus for mTOR (17). Several published
186 studies in mice and rats have also found that inhibiting mTOR protects against adenine-induced kidney disease (29-
187 31). The mTOR pathway is likely relevant to human DKD as a recent study found stimulation of mTOR activity in
188 kidney biopsies from patients with DKD (32) and our study with kidney biopsies from KPMP and CROCODILE
189 demonstrate that a number of outputs of mTOR are elevated in DKD. This includes pathways involved in bioenergetics
190 and pathways related to stimulation of extracellular matrix molecules. Further, adenine can increase the levels of
191 KIM1 and sTNFR1 demonstrating that adenine is likely an initiator of downstream injury and inflammatory markers.
192 Endogenous adenine production was blocked with a specific small molecule inhibitor of MTAP (MTDIA) and found
193 to protect against diabetic renal hypertrophy, elevation of kidney KIM1 and was protective of decline in kidney

194 function, as measured by serum cystatin C. It is possible that chronic MTAP inhibition with MTDIA could be
195 developed as a safe therapeutic as a prior study found that MTDIA extended lifespan in mice with colon cancer and
196 was provided for 294 days without evidence of toxicity (33). The role of adenine to accentuate mortality is not clear
197 although it is possible that adenine could be directly toxic to vascular cells.

198 The measure of UAdCR was closely associated with DKD progression in the non-macroalbuminuric diabetic
199 Pima Indian, CRIC, and SMART2D cohorts. As non-macroalbuminuric DKD leads to ESKD in many patients with
200 CKD and diabetes (7, 8, 34), the new UAdCR biomarker could be of clinical value to identify those patients likely to
201 progress. Further, the benefit of SGLT2 inhibitors may be due in part to reduce adenine levels as our study documented
202 that short term use of empagliflozin significantly attenuated the UAdCR.

203 Strengths of our study included multiple analysis of several independent cohorts across different ages, ethnicities
204 and stages of DKD. Additional strengths include application of spatial metabolomics and single cell transcriptomics
205 to identify a pathway linking adenine to mTOR in human kidney disease pathology and progression. Limitations of
206 our study was that the role of adenine was not demonstrated in type 1 DKD and other causes of CKD.

207 In conclusion, urine samples from independent well characterized cohorts of patients with diabetes identified the
208 UAdCR as a robust predictor of ESKD and mortality independent of albuminuria and baseline eGFR, and spatial
209 metabolomic and single cell transcriptomic studies from human kidney biopsies identified a potential role for
210 endogenous adenine and the mTOR pathway in DKD. Studies in cells and mice identified a causative role for adenine
211 and a small molecule therapeutic was found to block adenine production and was nephroprotective in a mouse model
212 of type 2 diabetes. Our results thus demonstrate that endogenous adenine could contribute to progressive kidney
213 disease in the context of type 2 diabetes.

214

215 **Methods**

216 *Clinical Cohorts.* Chronic Renal Insufficiency Cohort (CRIC): The parent CRIC Study recruited a racially diverse
217 group aged 21 to 74 years, ~50% with diabetes, with a broad range of kidney function (35). Informed consent was
218 obtained from participants; protocols were approved by Scientific and Data Coordinating Center). The current study
219 analyzed the urine sample at study entry (from baseline 24h urine samples) of 904 CRIC participants with diabetes
220 and eGFR between 20-70 mL/min/1.73 m² who had samples and outcomes data available. Singapore Study of Macro-
221 Angiopathy and microvascular Reactivity in Type 2 Diabetes cohort (SMART2D): SMART2D is an ongoing

222 prospective cohort study of Southeast Asian T2D participants recruited between 2011-2014 (36). Fasting spot urine
223 samples were collected at baseline and stored at -80°C. To validate findings from the CRIC cohort, 309 participants
224 with baseline eGFR 20-70 mL/min/1.73m² and urine ACR < 300 µg/mg were evaluated. All participants gave written
225 informed consent, and the study was approved by the Singapore National Healthcare Group. Pima Indians with early
226 DKD were enrolled in a randomized clinical trial (37) ([ClinicalTrials.gov](https://clinicaltrials.gov/ct2/show/study/NCT00340678) number, [NCT00340678](https://clinicaltrials.gov/ct2/show/study/NCT00340678)). GFR was
227 measured annually throughout the trial by the urinary clearance of iothalamate. Stored spot urine samples collected
228 for two consecutive years were available from 54 participants and included for analysis. Additionally, urine samples
229 were obtained under controlled euglycemic and hyperglycemic clamp conditions from a previously published clinical
230 study in patients with type 1 diabetes (T1D) without macroalbuminuria (n=42) to evaluate the effects of Empagliflozin
231 (Adjunctive-to-insulin and Renal Mechanistic (ATIRMA), NCT01392560) (38). Euglycemic clamp (4-6 mM glucose)
232 conditions were maintained for approximately 4 hours prior to urine collection. The following day hyperglycemia (9-
233 11 mM glucose) was maintained for 4 hours. Urine samples for adenine measurements were performed from samples
234 obtained at the 4-hour time point following euglycemia or hyperglycemia before and after empagliflozin (25 mg/d)
235 treatment for 8 weeks.

236 *Urine metabolomics (Zip-Chip Analysis).* Urine samples from Pima Indians, CRIC, SMART2D cohorts, and
237 ATIRMA urines were all analyzed using ZipChip (908 Devices, Boston, MA) coupled with mass spectrometry (39).
238 A rapid throughput urine adenine/creatinine assay was developed that showed excellent correlation with the gold
239 standard assay using LC-MS/MS (Supplementary Figure 1). The reportable linear range for urine adenine assay was
240 100 nM to 100 µM, with a limit of detection at 10 nM and coefficient of variation (CV)<10% across the reportable
241 linear range. Metabolite separation was achieved with a microfluidic chip which integrates capillary electrophoresis
242 (CE) with nano-electrospray ionization through a ZipChip interface. Data acquisition was performed with Q-Exactive
243 mass spectrometer (Thermo, San Jose, CA) and Thermo Scientific's software Xcalibur-Quan Browser for data
244 processing. Detailed procedures were previously published (39).

245 *Human kidney biopsies.* Human kidney samples were obtained *via* the Kidney Precision Medicine Project
246 (KPMP; The trial registration number from [ClinicalTrials.gov](https://clinicaltrials.gov/ct2/show/study/NCT04334707) is NCT04334707) and the Control of Renal Oxygen
247 Consumption, Mitochondrial Dysfunction, and Insulin Resistance (CROCODILE) studies (40-42). The KPMP and
248 CROCODILE studies were approved by the Institutional Review Board at Washington University, St. Louis, MO and
249 the University of Colorado, respectively, and written consent was obtained from all patients. Samples were frozen in

250 liquid nitrogen and stored at -80 °C until analysis. Snap frozen sample preparation and sectioning procedures for
251 MALDI-MSI were published at [dx.doi.org/10.17504/protocols.io.bcraiv2e](https://doi.org/10.17504/protocols.io.bcraiv2e).

252 *Animal studies.* Zucker Diabetic Fatty (ZDF) rat kidney and urine samples were provided by Epigen, Inc. to verify
253 that kidney spatial adenine correlated with the targeted urine adenine assay. C57Bl6J mice, db/m and db/db mice were
254 obtained from Jackson Labs. C57Bl6J mice were administered adenine for 4 weeks in drinking water before sacrificing
255 mice and harvesting tissues and blood samples after IACUC approval at UTHSA. db/m and db/db mice were
256 administered vehicle or methylthio-DADMe-Immucillin-A (MTDIA) MTAP inhibitor for a period of 8 weeks from
257 week 10 to week 18. Albumin ELISA kit (Cat. #, E101 and E90-134, Bethyl Laboratories Inc.) and creatinine
258 colorimetric kit (catalog ADI-907-030A, Enzo Life Sciences Inc.) were used for the urinary ACR. Serum cystatin C
259 was measured by Quantikine ELISA kit (Cat. #, MSCTC0, R&D systems). Plasma creatinine and metabolites in
260 kidney tissue were measured by the ZipChip-mass spectrometry as previously described (19). Urine and kidney KIM-
261 1 was measured by ELISA (Cat. #DY1817, R&D System).

262 *Mass Spectrometry Imaging (MSI) and Optical Imaging of Kidney Biopsies.* A multimodal imaging approach was
263 developed to investigate regional localization of metabolites in kidney sections. Bright-field (BF) and
264 autofluorescence (AF) microscopy outlined glomeruli and tubules, and PAS-H staining revealed regions of pathology
265 in serial sections. Matrix assisted laser desorption/ionization (MALDI)-MSI was performed with a Thermo Scientific
266 Q Exactive HF-X hybrid quadrupole-Orbitrap mass spectrometer (Thermo Scientific) in combination with a novel
267 elevated pressure MALDI/ESI interface (SpectroGlyph LLC, Kennewick, WA) (43). Metabolite annotation was
268 performed on METASPACE (44) and the optical image was uploaded to METASPACE and SCiLS Lab for visual
269 overlay of metabolites with optical images to provide an assessment of metabolites associated with normal-appearing
270 and pathologic features. Detailed procedures for MALDI-MSI are available at
271 [dx.doi.org/10.17504/protocols.io.bctfiwjn](https://doi.org/10.17504/protocols.io.bctfiwjn).

272 *Cell culture.* Human kidney proximal tubular (HK-2) cells were purchased from American Type Culture
273 Collection (Manassas, VA) and cultured as previously described (45). Murine kidney proximal tubular epithelial
274 (MCT) cells were cultured as previously described (46). Cells were treated with 20 μ M of adenine for the indicated
275 time points with and without rapamycin (Fisher Scientific). Phosphorylation of S6 kinase, ribosomal protein S6 and
276 expression of fibronectin and type 1 collagen $\alpha 2$ were analyzed by immunoblotting using antibodies against phosphor-
277 Thr389-S6 kinase (Cat. # 9205, Cell Signaling Technology), phosphor-Ser240/244 ribosomal protein S6 (Cat. #, 2215,

278 Cell Signaling Technology), ribosomal protein S6 (Cat. #, 2217, Cell Signaling Technology), MTAP (Cat. #, 62765,
279 Cell Signaling Technology), fibronectin (Cat. #, ab2413, Abcam Plc), type 1 collagen α 2 (Cat. #, 14695-1-AP,
280 Proteintech Group Inc), and beta-actin (Cat. #, A2066, Millipore Sigma).

281 *Statistical Analysis.* A composite kidney endpoint was defined as sustained kidney replacement therapy,
282 progression to GFR or eGFR $< 15 \text{ mL/min/1.73m}^2$, or $>50\%$ GFR or eGFR decline from baseline level. All-cause
283 mortality included death from any cause before reaching ESKD endpoint. Urine adenine was normalized to urine
284 creatinine concentrations and log₂ transformed. In the CRIC and SMART2D cohorts, the association of urine
285 adenine levels (tertile) with clinical endpoints was studied by multivariable Cox proportional hazard regression
286 models with adjustment for age, gender, ethnicity/race, body-mass index (BMI), hemoglobin A1c (HbA1c), mean
287 arterial pressure (MAP), baseline eGFR, and urine ACR (natural log-transformed) as covariates. The group with a
288 urine adenine/creatinine ratio in the lowest tertile was used as reference. Due to the limited number of cases in the
289 Pima Indian cohort we only reported univariate Cox proportional hazards analysis for this cohort. To evaluate the
290 pre-treatment and post-treatment effect of empagliflozin on urine adenine in the ATIRMA cohort, we performed a
291 linear regression analysis for repeated measures.

292 *Bioinformatic and systems medicine analysis.* Single cell transcriptomics and spatial metabolomics datasets
293 generated from healthy kidney tissue, unaffected tissue in kidney nephrectomy and biopsy samples (KPMP and
294 CROCODILE) were analyzed as recently described (40-42). The top pathway genes and proteins from the top 600
295 significant genes or proteins from proximal tubular cells were mapped onto pathways for subcellular processes using
296 the MBCO ontology (47).

297 *Study Approval.* For the CRIC study, Informed consent was obtained from participants; protocols were approved
298 by IRBs and Scientific and Data Coordinating Center. All participants gave written informed consent, and the study
299 was approved by the Singapore National Healthcare Group. The KPMP and CROCODILE studies were approved by
300 the Institutional Review Board at Washington University, St. Louis, MO and the University of Colorado, respectively,
301 and written consent was obtained from all patients.

302

303 **Author Contributions**

304 The first 9 coauthors each made unique and critical contributions to this manuscript, and authorship order was
305 determined after discussion among writing group members. KS, PB, SCL, JLL, RI, RGN, MK, and GZ designed the

306 study. KS, PB, SCL, DC and RGN acquired funding for the study. GZ, JH, HJL, RM, PB, JLL, HL, LH, PB, LK, VSS
307 acquired or generated the data. GZ, JH, HJL, JLL, HL, BC, LK and JG analyzed the data. KS, GZ, PB, MK, RGN and
308 RI wrote the manuscript. KS, PB, MK, SCL, LN, JZ, VS, BK, SW, JH, KT, BK, TF, HF, IB, JS, HDL, JS, RM, EO,
309 CA, TA, SCL, RGN, JG and RI provided scientific guidance and insights. All authors reviewed, edited, and approved
310 the manuscript.

311

312 **Conflicts of Interest**

313 K.S. reports serving as consultant for Visterra, Bayer, Sanofi, and receiving research support from Boehringer-
314 Ingelheim. K.S. also reports having equity in a startup company, SygnaMap. P.B. reports serving as a consultant for
315 AstraZeneca, Bayer, Bristol-Myers Squibb, Boehringer Ingelheim, Eli-Lilly, LG Chemistry, Sanofi, Novo Nordisk,
316 and Horizon Pharma. P.B. also serves on the advisory boards of AstraZeneca, Bayer, Boehringer Ingelheim, Novo
317 Nordisk, and XORTX. K.R.T. reports other support from Eli Lilly; personal fees and other support from Boehringer
318 Ingelheim; personal fees and other support from AstraZeneca; grants, personal fees and other support from Bayer AG;
319 grants, personal fees and other support from Novo Nordisk; grants and other support from Goldfinch Bio; other support
320 from Gilead; and grants from Travers outside the submitted work. R.G.N. and H.C.L. report no conflicts. J.H. reports
321 serving as a consultant for Maze Therapeutics, Chinook Therapeutics, Renalytix AI, and Seattle Genetics. D.C. has
322 received honoraria from Boehringer Ingelheim-Lilly, Merck, AstraZeneca, Sanofi, Mitsubishi-Tanabe, AbbVie,
323 Janssen, Bayer, Prometric, BMS, Maze, CSL Behring, and Novo Nordisk. H.L.H. has received honoraria for
324 participation in steering committees from AstraZeneca, Janssen, Eli-Lilly, Gilead, Bayer, Chinook, Novartis, and CSL
325 Behring; honoraria for participation in advisory boards from AstraZeneca, Vifor, Novartis, NovoNordisk, and Idorsia;
326 fees for consultancy from AstraZeneca, Travers Pharmaceuticals, Boehringer Ingelheim, and Novo Nordisk; and
327 research grant support from AstraZeneca, Janssen, Boehringer Ingelheim and NovoNordisk. Honoraria are paid to his
328 institution [University Medical Center Groningen].

329

330 **Acknowledgments**

331 G.Z, L.H., H.J.L, A.F, and K.S. receives salary and research support from NIH (UH3DK114920, 5U2CDK114886,
332 RO1DK110541). L.N., J.Z., B.K. were supported by NIDDK 5R01DK110541. J.J.L. receives research support from
333 Alexandra Health Fund (STAR grant 18203 and 20201). S.C.L. receives research support from Singapore National

334 Medical Research Council (MOH-000066, 0000714 and OFLCG/001/2017). P.B. receives salary and research
335 support from NIDDK (R01 DK129211, R21 DK129720, K23 DK116720, UC DK114886, and P30 DK116073), JDRF
336 (2-SRA-2019-845-S-B, 3-SRA-2017-424-M-B, 3-SRA-2022-1097-M-B), Boettcher Foundation, American Heart
337 Association (20IPA35260142), Ludeman Family Center for Women's Health Research at the University of Colorado,
338 the Department of Pediatrics, Section of Endocrinology and Barbara Davis Center for Diabetes at University of
339 Colorado School of Medicine. K.R.T. receives salary and research support from the NIDDK, NIMHD, NCATS, and
340 NHLBI (R01MD014712, U2CDK114886, UL1TR002319, U54DK083912, U01DK100846, OT2HL161847,
341 UM1AI109568) and the CDC (75D301-21-P-12254). R.G.N. was supported by the American Diabetes Association
342 (Clinical Science Award 1-08-CR-42) and R.G.N. and H.C.L. were supported by the Intramural Research Program of
343 NIDDK. J.H. and R.I. received salary support from U3CDK114886, R01GM137056, P01HL134605. Funding for the
344 CRIC Study was obtained under a cooperative agreement from National Institute of Diabetes and Digestive and
345 Kidney Diseases (U01DK060990, U01DK060984, U01DK061022, U01DK061021, U01DK061028, U01DK060980,
346 U01DK060963, U01DK060902 and U24DK060990). In addition, this work was supported in part by: the Perelman
347 School of Medicine at the University of Pennsylvania Clinical and Translational Science Award NIH/NCATS
348 UL1TR000003, Johns Hopkins University UL1 TR-000424, University of Maryland GCRC M01 RR-16500, Clinical
349 and Translational Science Collaborative of Cleveland, UL1TR000439 from the National Center for Advancing
350 Translational Sciences (NCATS) component of the National Institutes of Health and NIH roadmap for Medical
351 Research, Michigan Institute for Clinical and Health Research (MICHR) UL1TR000433, University of Illinois at
352 Chicago CTSA UL1RR029879, Tulane COBRE for Clinical and Translational Research in Cardiometabolic Diseases
353 P20 GM109036, Kaiser Permanente NIH/NCRR UCSF-CTSI UL1 RR-024131, Department of Internal Medicine,
354 University of New Mexico School of Medicine Albuquerque, NM R01DK119199. We acknowledge technical help
355 for animal studies from Richard Montellano, transcriptomics data organization from Fadhl AlAkwa and Philip
356 McCown, method development from Annapurna Pamreddy and data analysis by Rabiul Islam. D.C. has received
357 operational funding for clinical trials from Boehringer Ingelheim-Lilly, Merck, Janssen, Sanofi, AstraZeneca, and
358 Novo Nordisk.

359

360 **Appendix**

361 The author affiliations are as follows: the Center for Precision Medicine, the University of Texas Health San Antonio,
362 TX, USA (G.Z., A.F., L.H., H.J.L., M.A.V., C.A., J.G., K.S.), the Division of Nephrology, Department of Medicine,
363 the University of Texas Health San Antonio, TX, USA (G.Z., H.J.L., K.S.), the Department of Pharmacological
364 Sciences and Institute for Systems Biomedicine Icahn School of Medicine at Mount Sinai, New York, NY, USA
365 (J.H., R.I.), the Chronic Kidney Disease Section, National Institute of Diabetes and Digestive and Kidney Diseases,
366 Phoenix, AZ (H.C.L., R.G.N.), the Clinical Research Unit, Khoo Teck Puat Hospital, Singapore (J.J.L., S.C.L., J.G.),
367 the Department of Population Health Sciences, University of Texas Health San Antonio, 7703 Floyd Curl Drive, San
368 Antonio, TX, 78229, USA (R.F.), the SygnaMap, San Antonio, Texas, USA (L.H.), Audie L. Murphy Memorial VA
369 Hospital, South Texas Veterans Health Care System, San Antonio, TX, USA (G.Z., H.J.L., K.S.), the Department of
370 Pathology, University of Texas Health San Antonio, TX, USA (M.A.V.), the Department of Family Medicine and
371 Public Health, Herbert Wertheim School of Public Health, University of California-San Diego, La Jolla, California
372 (L.N.), the University of California-San Diego Moores Cancer Center, University of California-San Diego, La Jolla,
373 California (L.N., J.Z.), the Center for Molecular Medicine, Vienna, Austria (V.S.), the Department of Biostatistics,
374 Fielding School of Public Health, University of California, Los Angeles, California (B.K.), the Division of
375 Nephrology, Department of Medicine, Boston University, Boston, MA (S.W.), the Department of Medicine,
376 University of Washington, Seattle, WA, USA and the Division of Nephrology, Department of Medicine, Kidney
377 Research Institute, University of Washington, Seattle, Washington, USA (J.H., K.T., B.K., I.D.B.), the Division of
378 Nephrology, Department of Medicine and Section of Endocrinology, Department of Pediatrics, University of Colorado
379 Anschutz Medical Campus, Aurora, CO, USA (P.B.), the Institute of Molecular Systems Biology, ETH Zurich, 8093,
380 Zurich, Switzerland (T.F.), the Center for Clinical Epidemiology and Biostatistics, Perelman School of Medicine at the
381 University of Pennsylvania and the Department of Biostatistics, Epidemiology, and Informatics, Perelman School of
382 Medicine at the University of Pennsylvania (H.F.), the Epigen Biosciences, Inc., San Diego, California, USA (F.C.T.),
383 the Cleveland Clinic, Cleveland, Ohio (J.S.), Department of Clinical Pharmacy and Pharmacology, University of
384 Groningen, University Medical Center Groningen, Groningen, the Netherlands (H.L.H.), The George Institute for
385 Global Health, Sydney, Australia (H.L.H.), the Department of Internal Medicine, University of Michigan, Ann Arbor,
386 Michigan, USA (R.M., E.O., J.H., M.K.), the Environmental Molecular Sciences Laboratory, Pacific Northwest
387 National Laboratory, Richland, WA, USA (C.A.), the Structural and Computational Biology Unit, European
388 Molecular Biology Laboratory, Heidelberg, Germany (T.A.), the Diabetes Center, Admiralty Medical Center,

389 Singapore and the Saw Swee Hock School of Public Health, National University of Singapore, Singapore and the Lee
390 Kong Chian School of Medicine, Nanyang Technological University, Singapore (S.C.L.)

391

392

393

394

395

396

397

398

399

400

401

402

403

404

405

406

407

408

409

410

411

412

413

414

415 **References**

- 416 1. Nath KA. Tubulointerstitial changes as a major determinant in the progression of renal damage. *Am J Kidney Dis.*
417 1992;20(1):1-17.
- 418 2. Di Vincenzo A, Bettini S, Russo L, Mazzocut S, Mauer M, and Fioretto P. Renal structure in type 2 diabetes:
419 facts and misconceptions. *J Nephrol.* 2020;33(5):901-7.
- 420 3. Mauer SM, Steffes MW, and Brown DM. The kidney in diabetes. *Am J Med.* 1981;70(3):603-12.
- 421 4. Caramori ML, Parks A, and Mauer M. Renal lesions predict progression of diabetic nephropathy in type 1
422 diabetes. *J Am Soc Nephrol.* 2013;24(7):1175-81.
- 423 5. Yamanouchi M, Furuichi K, Hoshino J, Ubara Y, and Wada T. Nonproteinuric diabetic kidney disease. *Clinical*
424 *and experimental nephrology.* 2020;24(7):573-81.
- 425 6. Berhane AM, Weil EJ, Knowler WC, Nelson RG, and Hanson RL. Albuminuria and estimated glomerular
426 filtration rate as predictors of diabetic end-stage renal disease and death. *Clin J Am Soc Nephrol.* 2011;6(10):2444-
427 51.
- 428 7. Porrini E, Ruggenenti P, Mogensen CE, Barlovic DP, Praga M, Cruzado JM, et al. Non-proteinuric pathways in
429 loss of renal function in patients with type 2 diabetes. *Lancet Diabetes Endocrinol.* 2015;3(5):382-91.
- 430 8. Pichaiwong W, Homsuwan W, and Leelahavanichkul A. The prevalence of normoalbuminuria and renal
431 impairment in type 2 diabetes mellitus. *Clin Nephrol.* 2019;92(2):73-80.
- 432 9. Caramori ML, Fioretto P, and Mauer M. The need for early predictors of diabetic nephropathy risk: is albumin
433 excretion rate sufficient? *Diabetes.* 2000;49(9):1399-408.
- 434 10. Forst T, Mathieu C, Giorgino F, Wheeler DC, Papanas N, Schmieder RE, et al. New strategies to improve clinical
435 outcomes for diabetic kidney disease. *BMC Med.* 2022;20(1):337.
- 436 11. Tuttle KR, Agarwal R, Alpers CE, Bakris GL, Brosius FC, Kolkhof P, et al. Molecular mechanisms and
437 therapeutic targets for diabetic kidney disease. *Kidney Int.* 2022;102(2):248-60.
- 438 12. Zhang J, Fuhrer T, Ye H, Kwan B, Montemayor D, Tumova J, et al. High-Throughput Metabolomics and Diabetic
439 Kidney Disease Progression: Evidence from the Chronic Renal Insufficiency (CRIC) Study. *Am J Nephrol.*
440 2022:1-11.
- 441 13. Rahman A, Yamazaki D, Sufiun A, Kitada K, Hitomi H, Nakano D, et al. A novel approach to adenine-induced
442 chronic kidney disease associated anemia in rodents. *Plos One.* 2018;13(2):e0192531.

- 443 14. Diwan V, Brown L, and Gobe GC. Adenine-induced chronic kidney disease in rats. *Nephrology (Carlton)*.
444 2018;23(1):5-11.
- 445 15. Claramunt D, Gil-Pena H, Fuente R, Hernandez-Frias O, and Santos F. Animal models of pediatric chronic kidney
446 disease. Is adenine intake an appropriate model? *Nefrologia : publicacion oficial de la Sociedad Espanola*
447 *Nefrologia*. 2015;35(6):517-22.
- 448 16. Schiaffino S, Reggiani C, Akimoto T, and Blaauw B. Molecular Mechanisms of Skeletal Muscle Hypertrophy. *J*
449 *Neuromuscul Dis*. 2021;8(2):169-83.
- 450 17. Hoxhaj G, Hughes-Hallett J, Timson RC, Ilagan E, Yuan M, Asara JM, et al. The mTORC1 Signaling Network
451 Senses Changes in Cellular Purine Nucleotide Levels. *Cell Rep*. 2017;21(5):1331-46.
- 452 18. Lubin M, and Lubin A. Selective killing of tumors deficient in methylthioadenosine phosphorylase: a novel
453 strategy. *Plos One*. 2009;4(5):e5735.
- 454 19. Zhang J, Fuhrer T, Ye H, Kwan B, Montemayor D, Tumova J, et al. High-Throughput Metabolomics and Diabetic
455 Kidney Disease Progression: Evidence from the Chronic Renal Insufficiency (CRIC) Study. *Am J Nephrol*.
456 2022;53(2-3):215-25.
- 457 20. Perkins BA, Ficociello LH, Silva KH, Finkelstein DM, Warram JH, and Krolewski AS. Regression of
458 microalbuminuria in type 1 diabetes. *N Engl J Med*. 2003;348(23):2285-93.
- 459 21. Niewczas MA, Pavkov ME, Skupien J, Smiles A, Md Dom ZI, Wilson JM, et al. A signature of circulating
460 inflammatory proteins and development of end-stage renal disease in diabetes. *Nat Med*. 2019;25(5):805-13.
- 461 22. Tofte N, Lindhardt M, Adamova K, Bakker SJL, Beige J, Beulens JWJ, et al. Early detection of diabetic kidney
462 disease by urinary proteomics and subsequent intervention with spironolactone to delay progression
463 (PRIORITY): a prospective observational study and embedded randomised placebo-controlled trial. *Lancet*
464 *Diabetes Endocrinol*. 2020;8(4):301-12.
- 465 23. Sharma K, Karl B, Mathew AV, Gangoiti JA, Wassel CL, Saito R, et al. Metabolomics reveals signature of
466 mitochondrial dysfunction in diabetic kidney disease. *J Am Soc Nephrol*. 2013;24(11):1901-12.
- 467 24. Looker HC, Mauer M, and Nelson RG. Role of Kidney Biopsies for Biomarker Discovery in Diabetic Kidney
468 Disease. *Adv Chronic Kidney Dis*. 2018;25(2):192-201.

- 469 25. de Frutos S, Luengo A, Garcia-Jerez A, Hatem-Vaquero M, Griera M, O'Valle F, et al. Chronic kidney disease
470 induced by an adenine rich diet upregulates integrin linked kinase (ILK) and its depletion prevents the disease
471 progression. *Biochim Biophys Acta Mol Basis Dis.* 2019;1865(6):1284-97.
- 472 26. George SA, Al-Rushaidan S, Francis I, Soonowala D, and Nampoory MRN. 2,8-Dihydroxyadenine Nephropathy
473 Identified as Cause of End-Stage Renal Disease After Renal Transplant. *Exp Clin Transplant.* 2017;15(5):574-7.
- 474 27. Mo Y, Sun H, Zhang L, Geng W, Wang L, Zou C, et al. Microbiome-Metabolomics Analysis Reveals the
475 Protection Mechanism of alpha-Ketoacid on Adenine-Induced Chronic Kidney Disease in Rats. *Front Pharmacol.*
476 2021;12:657827.
- 477 28. Saleh MA, Awad AM, Ibrahim TM, and Abu-Elsaad NM. Small-Dose Sunitinib Modulates p53, Bcl-2, STAT3,
478 and ERK1/2 Pathways and Protects against Adenine-Induced Nephrotoxicity. *Pharmaceuticals (Basel).*
479 2020;13(11).
- 480 29. Wang J, Chai L, Lu Y, Lu H, Liu Y, and Zhang Y. Attenuation of mTOR Signaling Is the Major Response
481 Element in the Rescue Pathway of Chronic Kidney Disease in Rats. *Neuroimmunomodulation.* 2020;27(1):9-18.
- 482 30. Nakano T, Watanabe H, Imafuku T, Tokumaru K, Fujita I, Arimura N, et al. Indoxyl Sulfate Contributes to
483 mTORC1-Induced Renal Fibrosis via The OAT/NADPH Oxidase/ROS Pathway. *Toxins (Basel).* 2021;13(12).
- 484 31. Zhao Y, Zhao MM, Cai Y, Zheng MF, Sun WL, Zhang SY, et al. Mammalian target of rapamycin signaling
485 inhibition ameliorates vascular calcification via Klotho upregulation. *Kidney Int.* 2015;88(4):711-21.
- 486 32. Schaub JA, AlAkwa FM, McCown PJ, Naik AS, Nair V, Eddy S, et al. SGLT2 inhibitors mitigate kidney tubular
487 metabolic and mTORC1 perturbations in youth-onset type 2 diabetes. *J Clin Invest.* 2023;133(5).
- 488 33. Firestone RS, Feng M, Basu I, Peregrina K, Augenlicht LH, and Schramm VL. Transition state analogue of MTAP
489 extends lifespan of APC(Min/+) mice. *Sci Rep.* 2021;11(1):8844.
- 490 34. Liyanage P, Lekamwasam S, Weeraratna TP, and Srikantha D. Prevalence of normoalbuminuric renal
491 insufficiency and associated clinical factors in adult onset diabetes. *BMC Nephrol.* 2018;19(1):200.
- 492 35. Yaffe K, Ackerson L, Tamura MK, Le Blanc P, Kusek JW, Sehgal AR, et al. Chronic Kidney Disease and
493 Cognitive Function in Older Adults: Findings from the Chronic Renal Insufficiency Cohort Cognitive Study.
494 *Journal of the American Geriatrics Society.* 2010;58(2):338-45.

- 495 36. Pek SL, Tavintharan S, Wang X, Lim SC, Woon K, Yeoh LY, et al. Elevation of a novel angiogenic factor,
496 leucine-rich-alpha2-glycoprotein (LRG1), is associated with arterial stiffness, endothelial dysfunction, and
497 peripheral arterial disease in patients with type 2 diabetes. *J Clin Endocrinol Metab.* 2015;100(4):1586-93.
- 498 37. Weil EJ, Fufaa G, Jones LI, Lovato T, Lemley KV, Hanson RL, et al. Effect of losartan on prevention and
499 progression of early diabetic nephropathy in American Indians with type 2 diabetes. *Diabetes.* 2013;62(9):3224-
500 31.
- 501 38. Škrtić M, Yang GK, Perkins BA, Soleymannlou N, Lytvyn Y, von Eynatten M, et al. Characterisation of glomerular
502 haemodynamic responses to SGLT2 inhibition in patients with type 1 diabetes and renal hyperfiltration.
503 *Diabetologia.* 2014;57(12):2599-602.
- 504 39. Liu H, Sridhar VS, Montemayor D, Lovblom LE, Lytvyn Y, Ye H, et al. Changes in plasma and urine metabolites
505 associated with empagliflozin in patients with type 1 diabetes. *Diabetes, obesity & metabolism.*
506 2021;23(11):2466-75.
- 507 40. Lake BB, Chen S, Hoshi M, Plongthongkum N, Salamon D, Knoten A, et al. A single-nucleus RNA-sequencing
508 pipeline to decipher the molecular anatomy and pathophysiology of human kidneys. *Nat Commun.*
509 2019;10(1):2832.
- 510 41. Menon R, Otto EA, Hoover P, Eddy S, Mariani L, Godfrey B, et al. Single cell transcriptomics identifies focal
511 segmental glomerulosclerosis remission endothelial biomarker. *JCI Insight.* 2020;5(6).
- 512 42. Hansen J, Sealfon R, Menon R, Eadon MT, Lake BB, Steck B, et al. A reference tissue atlas for the human kidney.
513 *Science advances.* 2022;8(23):eabn4965.
- 514 43. Belov ME, Ellis SR, Dilillo M, Paine MRL, Danielson WF, Anderson GA, et al. Design and Performance of a
515 Novel Interface for Combined Matrix-Assisted Laser Desorption Ionization at Elevated Pressure and Electrospray
516 Ionization with Orbitrap Mass Spectrometry. *Anal Chem.* 2017;89(14):7493-501.
- 517 44. Palmer A, Phapale P, Chernyavsky I, Lavigne R, Fay D, Tarasov A, et al. FDR-controlled metabolite annotation
518 for high-resolution imaging mass spectrometry. *Nature methods.* 2017;14(1):57-60.
- 519 45. Yang L, Besschetnova TY, Brooks CR, Shah JV, and Bonventre JV. Epithelial cell cycle arrest in G2/M mediates
520 kidney fibrosis after injury. *Nat Med.* 2010;16(5):535-43, 1p following 143.

- 521 46. Lee HJ, Lee DY, Mariappan MM, Feliens D, Ghosh-Choudhury G, Abboud HE, et al. Hydrogen sulfide inhibits
522 high glucose-induced NADPH oxidase 4 expression and matrix increase by recruiting inducible nitric oxide
523 synthase in kidney proximal tubular epithelial cells. *J Biol Chem.* 2017;292(14):5665-75.
- 524 47. Hansen J, Meretzky D, Woldesenbet S, Stolovitzky G, and Iyengar R. A flexible ontology for inference of
525 emergent whole cell function from relationships between subcellular processes. *Sci Rep.* 2017;7(1):17689.
- 526
- 527

528 **Table 1.** Baseline characteristics of patients with diabetes in the Pima American Indians, CRIC and SMART2D
 529 studies.
 530

Characteristics	Pima cohort (N=54)	CRIC cohort (N=904)	SMART2D cohort (N=309)
	Mean ± SD/N (%)	Mean ± SD/N (%)	Mean ± SD/N (%)
Index age (years)	45.1 ± 9.6	60 ± 9.4	64.5 ± 9.6
Sex			
Male	13 (24%)	515 (57%)	176 (57%)
Female	41 (76%)	390 (43%)	133 (43%)
		Black: 376 (41%)	
Ethnicity (%)	American Indian: 54 (100%)	Hispanic: 141 (16%)	Chinese: 163 (53%)
		Other: 37 (4%)	Malay: 71 (23%)
		White: 350 (39%)	Asian Indian: 75 (24%)
Current smoker			
Yes	..	510 (56%)	20 (7%)
No	..	391 (43%)	289 (93%)
Body mass index (kg/m ²)	35.4 ± 7.1	34 ± 7.8	27.7 ± 5.3
HbA1c (%)	9.6 ± 2	7.6 ± 1.6	7.6 ± 1.3
Mean artery pressure (mmHg)	93.2 ± 10	90 ± 13	98 ± 11
eGFR* mL/min/1.73m ²)	139 ± 49	40 ± 12	53 ± 13
ACR** (median (IQR), mg/g)	40 (15 -164)	116 (16 - 756)	27 (11- 87)
ACR category (N,%)***			
< 30 mg/g	26 (48%)	298 (33%)	162 (52%)
30-300 mg/g	16 (30%)	260 (28%)	147 (48%)
>300 mg/g	12 (22%)	341 (39%)	..

531
 532 BMI, body mass index; eGFR, estimated glomerular filtration rate; HbA1c, hemoglobin A1c; UACR, urine albumin-
 533 to-creatinine ratio; *data for Pima cohort is measured GFR in ml/min; **Continuous ACR is summarized using
 534 median (IQR, interquartile range) because of its skewed distribution. ***data for CRIC cohort is based on 24h urine
 535 albumin or albumin/creatinine values. For ACR category and all other continuous variables are summarized using
 536 mean ± SD.

537
 538
 539
 540
 541

542 **Table 2.** Association of baseline urine adenine/creatinine ratio (UAdCR) with risk for progression to ESKD and all-
543 cause mortality in CRIC and SMART2D participants with type 2 diabetes with 7 years follow up.

544

Adenine/Creatinine ratio	CRIC cohort (N=889)		SMART2D cohort (N=309)	
	HR (95% CI)	p value	HR (95% CI)	p value
1-SD increment	1.15 (1.03-1.28)	0.010	1.48 (1.15-1.90)	0.003
Tertile 2 vs tertile 1	1.59 (1.21-2.09)	<0.001	0.81 (0.44-1.50)	0.502
Tertile 3 vs tertile 1	1.57 (1.18-2.10)	0.002	1.77 (1.00-3.12)	0.048

545

546 Multivariate Cox proportional hazard regression models were adjusted for baseline age, sex, ethnicity, body mass
547 index, mean arterial pressure, hemoglobin A1c, eGFR and natural-log transformed urine albumin/creatinine ratio.
548 UAdCR was modelled as both continuous variable (1-SD increment in log₂-transformed adenine/creatinine ratio) and
549 categorical variable (low tertile as reference). There were 15 subjects in CRIC with missing values for the clinical co-
550 variates.

551

552

553

554

555

556

557

558

559

560

561

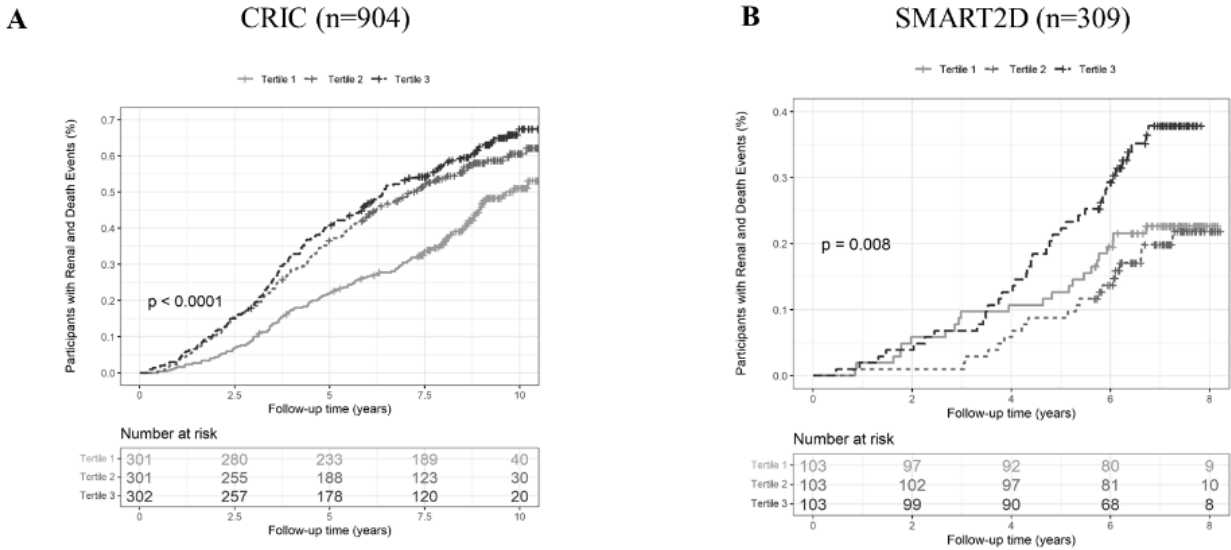
562

563

564

565

566



567

568

569 **Figure 1. High urine adenine/creatinine (UAdCR) levels identify patients with diabetes who are at high risk of**

570 **end stage kidney disease (ESKD) and mortality.** Participants with diabetes in the Chronic Renal Insufficiency

571 Cohort (CRIC) cohort (n=904) had UAdCR measured within 1 year of enrollment and followed for 10 years. The

572 participants in the top tertile had the highest risk of ESKD and all cause mortality (A). Participants from the Singapore

573 Study of Macro-Angiopathy and microvascular Reactivity in Type 2 Diabetes (SMART2D) study (n=309) had

574 UAdCR measurements at the time of enrollment and were followed for 7 years. The participants in the top tertile for

575 UAdCR had the highest risk for ESKD and all-cause mortality.

576

577

578

579

580

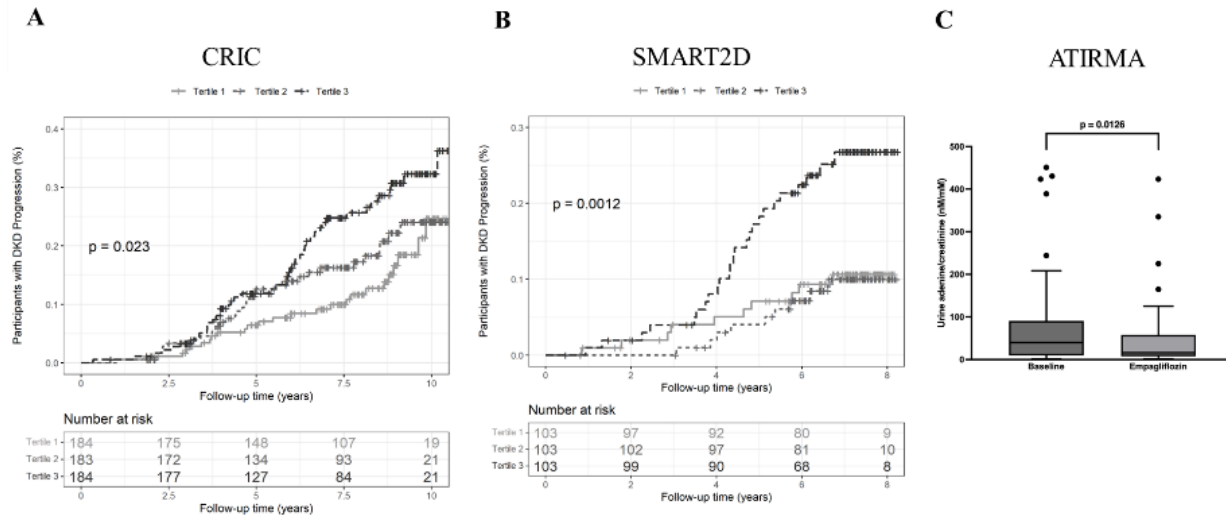
581

582

583

584

585



586

587 **Figure 2. High urine adenine/creatinine (UAdCR) tertile identifies end stage kidney disease (ESKD) outcome**

588 **in non-macroalbuminuric patients with diabetes and empagliflozin reduced urine adenine/creatinine ratio.** The

589 participants with the top UAdCR tertile had a significant increase in risk of ESKD from CRIC (n=551) (A) and

590 SMART2D (n=309) (B) studies. Patients with T1 diabetes underwent treatment with empagliflozin for 8 weeks which

591 reduced UAdCR levels (n=40 patients) (C).

592

593

594

595

596

597

598

599

600

601

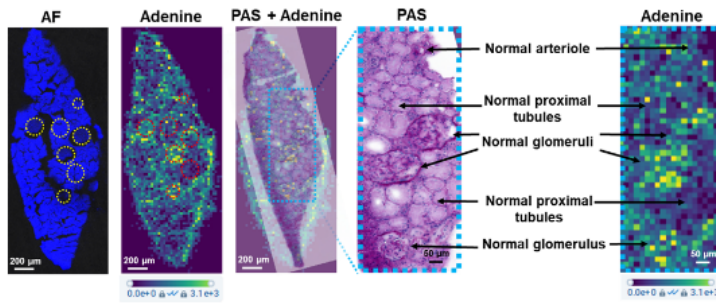
602

603

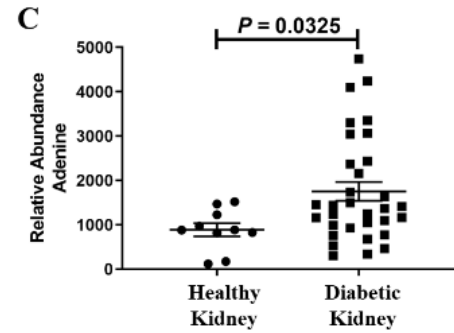
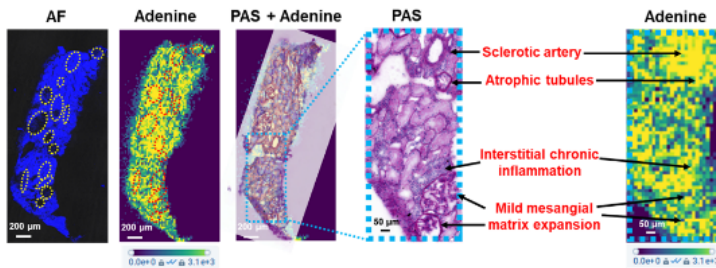
604

605

A. Healthy control kidney biopsy



B. Diabetic kidney biopsy



606

607 **Figure 3. Spatial metabolomics identifies adenine in regions of pathology in non-macroalbuminuric patients**

608 **with diabetes.** Adenine was localized to regions of normal glomeruli and vessels in the normal kidney (A). In a

609 diabetic kidney, adenine is diffusely increased across the tissue section and prominent in regions of sclerotic blood

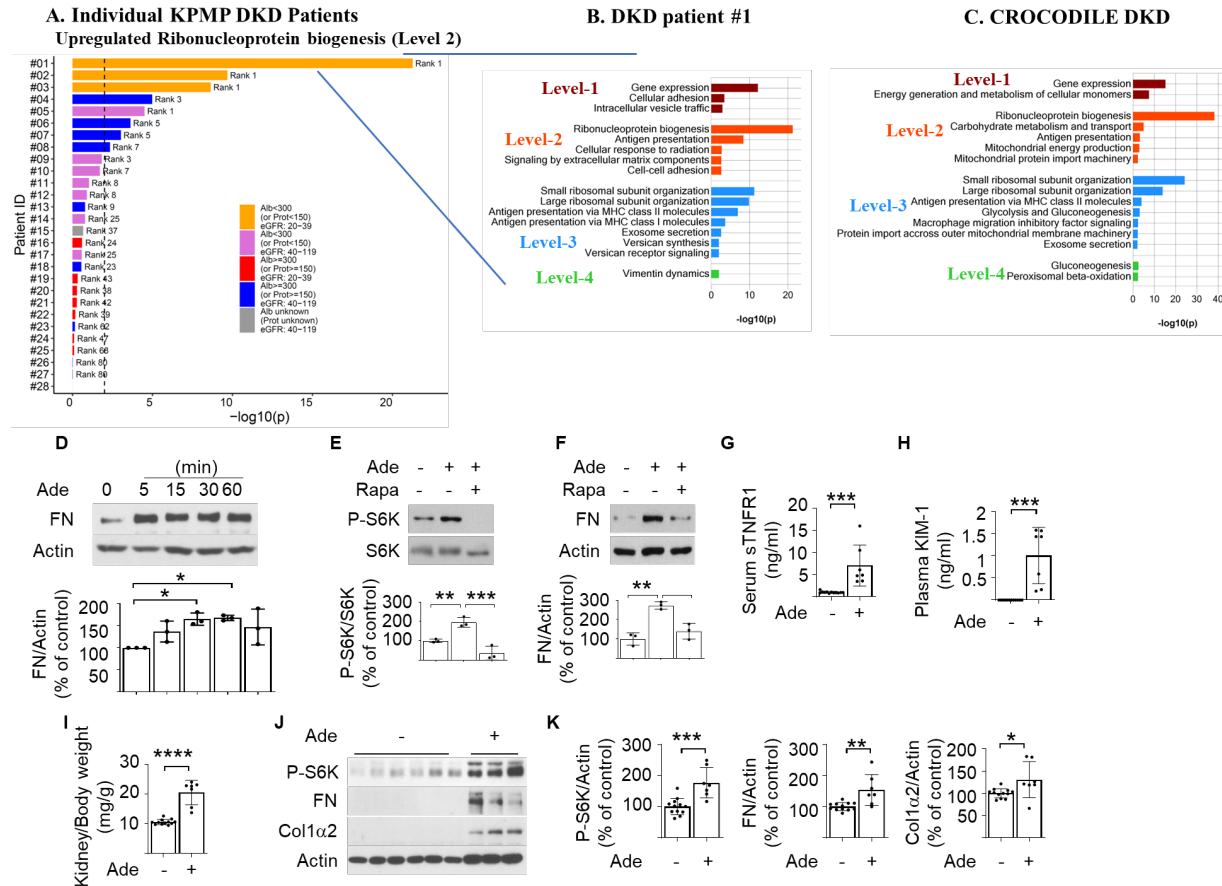
610 vessels, glomeruli with mild sclerosis and regions of atrophic tubules and interstitial inflammation (B). Quantitative

611 assessment across healthy controls (n=5 from Control of Renal Oxygen Consumption, Mitochondrial Dysfunction and

612 Insulin Resistance (CROCODILE) study) and diabetic samples (n=8 T1D from CROCODILE and n=8 T2D (2 from

613 CROCODILE and 6 from Kidney Precision Medicine Project (KPMP)) demonstrates a statistically significant

614 increase of adenine in kidney tissue sections (C).



615
616 **Figure 4. Molecular pathways and events implicating ribonucleoprotein biogenesis and mammalian target of**
617 **rapamycin (mTOR) pathway with adenine in diabetic kidney disease (DKD):** Protein synthesis
618 (Ribonucleoprotein (RNP) biogenesis) pathway increased in proximal tubule cells of DKD patients without
619 proteinuria (A) Single cell- transcriptomic data obtained from DKD kidney biopsies for the Kidney Precision Medicine
620 Project (KPMP) was analyzed for differentially expressed genes in proximal tubule (PT) of each DKD patient versus
621 healthy reference tissue. Upregulated genes with an adjusted p-value ≤ 0.01 and ranked among the top 600 significant
622 DEGs were subjected to pathway enrichment analysis using the Molecular Biology of the Cell Ontology (MBCO).
623 Ranking for the RNP biogenesis pathway (a Level 2 pathway canonically regulated by the mTOR pathway) is shown
624 for 28 individual patients. Vertical dashed line indicates p value ≤ 0.01 for pathway ranking (B) Up to top five, five,
625 ten and five level-1 (dark red), level-2 (red), level-3 (blue) and level-4 (green) pathways using MBCO are shown for
626 patient #1 (p-value ≤ 0.01). See blue lines from A to B. Single cell transcriptomic data from T2D patients (N=6) with
627 low albuminuria compared to cohort specific healthy samples was analyzed to identify upregulated pathways in PT
628 cells (C). Note that the RNP biogenesis pathway is the top ranked Level-2 pathway in both independent studies. Cell

629 culture studies in mouse proximal tubular cells demonstrated an increase in fibronectin (D), phospho-S6 kinase and
630 mediation of fibronectin (FN) upregulation is blocked by rapamycin (E, F), indicating mTOR mediates adenine effect.
631 Adenine administration to mice increases serum soluble tumor necrosis factor-1 (sTNFR1) (G), plasma kidney injury
632 marker-1 (KIM-1) (H), stimulates kidney (I) and matrix molecules in the kidney (J, K) (n=12 in control group and
633 n=7 in adenine treated group, *p<0.05, **p<0.01, ***p<0.001, ****p<0.0001).

634

635

636

637

638

639

640

641

642

643

644

645

646

647

648

649

650

651

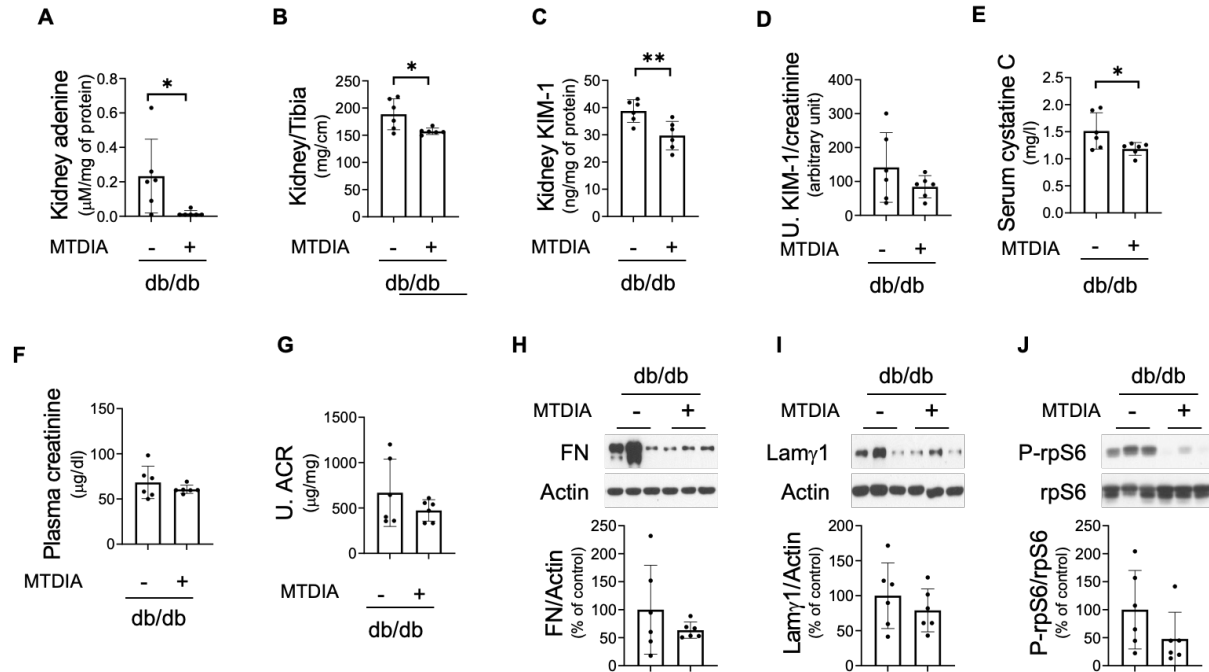
652

653

654

655

656



657

658 **Figure 5. Methylothioadenosine phosphorylase (MTAP) inhibitor ameliorates kidney injury in db/db mice**

659 **with type 2 diabetes:** Methylthio-DADMe-Immucillin-A (MTDIA) significantly reduced kidney adenine levels

660 (A), kidney hypertrophy (B), kidney KIM-1 levels (C) in diabetic mice. MTDIA significantly reduced diabetes-

661 increased serum cystatin C (E), and partially reduced plasma creatinine (F), and albuminuria (G) in diabetic mice.

662 Diabetes induced kidney matrix protein levels were partially reduced by MTDIA (H, I). Ribosomal S6

663 phosphorylation was partially reduced by MTDIA in the kidney of db/db mice (J) (n=6 per group, *p<0.05,

664 **p<0.01, ***p<0.001).

665

666

667

668

669 **Supplementary Figures and Tables**

670 **Supplementary Table 1.** Hazard Ratios of ESKD or >50% decline in GFR incidence between tertiles of urine
671 adenine/creatinine ratio (UAdCR) in Pima cohort without macroalbuminuria.

672

Pima American Indians	N	Continuous			T2 vs T1			T3 vs T1		
		HR	95% CI	P value	HR	95% CI	P value	HR	95% CI	P value
No macroalbuminuria	42	1.89	1.18-3.03	0.008	1.66	0.54-5.09	0.37	4.57	1.57-13.44	0.006

673

674 HR = hazard ratio; CI = confidence interval; No macroalbuminuria (ACR <300 mg/g). T1 = lowest tertile of UAdCR,
675 T2=middle tertile of UAdCR and T3 = highest tertile of UAdCR. For the continuous measure of UAdCR, HR is per
676 standard deviation in natural log-transformed UAdCR.

677

678

679

680

681

682

683

684

685

686

687

688

689

690

691

692

693

694 **Supplementary Table 2.** Association of baseline urine adenine/creatinine ratio (UAdCR) with risk for progression to
695 ESKD in CRIC and SMART2D participants with non-macroalbuminuria and type 2 diabetes with 7 year follow up.

Adenine/Creatinine ratio	CRIC cohort (N=551)		SMART2D cohort (N=309)	
	HR (95% CI)	p value	HR (95% CI)	p value
1-SD increment	1.37 (1.08-1.73)	0.011	1.70 (1.21-2.39)	0.002
Tertile 2 vs tertile 1	1.96 (1.06-3.60)	0.031	0.91 (0.37-2.28)	0.848
Tertile 3 vs tertile 1	2.36 (1.26-4.39)	0.006	2.39 (1.08-5.29)	0.032

696
697 Multivariate Cox proportional hazard regression models were adjusted for baseline age, sex, ethnicity, body mass
698 index, mean arterial pressure, hemoglobin A1c, eGFR and natural-log transformed urine albumin/creatinine ratio.
699 UAdCR was modelled as both continuous variable (1-SD increment in log2-transformed adenine/creatinine ratio) and
700 categorical variable (low tertile as reference). There were 7 subjects in CRIC with missing values for the clinical co-
701 variates.

702

703

704

705

706

707

708

709

710

711

712

713

714

715

716

717

718

719 **Supplement Table 3.** Correlations between urine adenine/creatinine ratio (UAdCR) and urine albumin/creatinine
720 ratio (UACR) or the estimated glomerular filtration rate (eGFR) in the non-macro groups from CRIC and SMART2D.

721

Cohort	UACR (r, p-value)	eGFR (r, p-value)
CRIC (n=551)	r=-0.02, p=0.62	r=0.01, p=0.74
SMART2D (n=309)	r=0.01, p=0.82	r=-0.06, p=0.28

722

723

724

725

726

727

728

729

730

731

732

733

734

735

736

737

738

739

740

741

742

743

744

745

746 **Supplementary Table 4.** Baseline characteristics of participants in ATIRMA, KPMP, and CROCODILE studies.

	ATIRMA (n=40)	KPMP (n=54)	CROCODILE (n=15)
Characteristics			
Age, years	24.3 ± 5.1	(50.5 - 59.5) ± 12.7	24.1 ± 3.9
Sex			
Male, n (%)	20 (50.0)	22 (40)	7 (46.7)
Weight, kg	71.3 ± 12.6	..	73.5 ± 12.7
BMI, kg/m ²	24.1 ± 3.2	..	25.2 ± 3.9
HRT, n (%)	..	20 (36.4)	5 (33.3)
T1D, n (%)	..	4 (7.3)	8 (51.3)
T2D, n (%)	..	30 (56.4)	2 (13.3)
HbA1C (%)	7.8 ± 0.9	..	.
MAP, mmHg	79.5 ± 7.4	..	.
eGFR*, mL/min/1.73m ²	149.8 ± 33.9	(50.6 - 59.6) ± 23.6	148.8 ± 34.6
Urine ACR (mg/g)	10.35 ± 5.93	..	7.8 ± 7.9

747

748 BMI: body-mass index, SBP: systolic blood pressure, DBP: diastolic blood pressure, MAP: mean arterial pressure,

749 GFR: glomerular filtration rate, ERPF: estimated renal plasma flow, HbA1C: glycated hemoglobin A1c. (values

750 expressed as Mean ± SD)

751

752

753

754

755

756

757

758

759

760

761

762

763

764

765 **Supplementary Table 5.** Correlation of urine adenine/creatinine ratio (UAdCR) with tissue levels of adenine.

Spatial Adenine	Correlation with Urine Adenine/Creatinine with Kidney Adenine by MALDI-MSI
Glom Adenine	R = 0.64, p<0.001
Non-Glom Adenine	R = 0.81, p<0.001
Whole Slide Image Adenine	R = 0.73, p<0.001

766

767 Correlation of UAdCR measurements with tissue levels of adenine by spatial metabolomics of rat kidney samples

768 (n=9).

769

770 **Supplementary Table 6. Clinical parameter in MTDIA treated db/db mice with type 2 diabetes**

	db/m	db/m + MTDIA	db/db	db/db + MTDIA
	(n=6)	(n=6)	(n=6)	(n=6)
Parameters				
Body weight (g)	29.0 ±2.0	28.9 ±0.3	45.0 ±4.6	43.1 ±8.8
Blood glucose (mg/dL)	121.7 ±8.3	142.4 ±38.3	477.0 ±137.8	409.0 ±150.8
Food intake (g/mouse/day)	4.6 ±0.9	5.4 ±1.7	5.8 ±0.6	5.5 ±1.1
Water intake (g/mouse/day)	4.3 ± 0.8	4.5 ±1.0	9.7 ±3.6	8.2 ±2.7

771

772

773

774

775

776

777

778

779

780

781

782

783

784

785

786

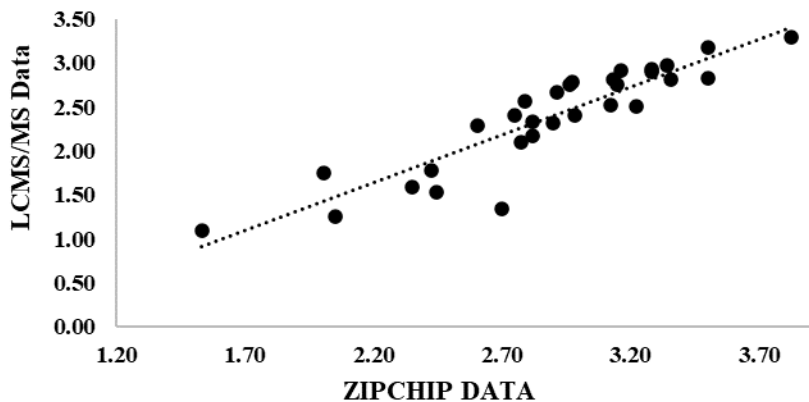
787

788

789 **Supplementary Table 7. Kidney metabolites in MTDIA treated db/db mice with type 2 diabetes**

Metabolites (mM/mg of protein)	db/db (mean ± SD)	db/db + MTDIA (mean ± SD)
Alanine	210 ±28.2	252 ±69.1
Arginine	25 ±5.6	29 ±9.9
Asparagine	54 ±12.9	64 ± 17.0
Aspartic acid	188 ±26.9	177 ±27.3
Cysteine	88 ±10.4	85 ±13.1
Glutamic acid	584 ±55.2	536 ±59.6
Glutamine	124 ±14.5	124 ±31.4
Glycine	472 ±38.7	514 ±82.4
Histidine	21 ±4.4	25 ±10.2
Isoleucine	25 ±4.0	35 ±13.3
Leucine	60 ±10.0	81 ±30.9
Lysine	35 ±9.0	46 ±19.3
Methionine	25 ±5.0	31 ±11.0
Phenylalanine	27 ±6.6	28 ±8.2
Proline	44 ±9.9	66 ±34.8
Serine	96 ±21.3	125 ±48.4
Threonine	56 ±10.1	72 ±27.1
Tryptophan	6 ±1.4	8 ±2.6
Tyrosine	35 ±7.0	47 ±17.8
Valine	46 ±6.7	64 ±24.0
3- hydroxykynurenine	N.D.	N.D.
Betaine	118 ±54.5	152 ±67.0
DL-homocysteine	N.D.	N.D.
GABA	3 ±0.6	9 ±9.2
Glycyl-histidine	0.13 ±0.03	0.15 ±0.05
Kynurenine	N.D.	N.D.
L-a-aminobutyric acid	0.85 ±0.77	0.62 ±0.26
Nicotinic acid	N.D.	N.D.
Ornithine	5 ±1.7	11 ±7.6
Pipecolate	0.66 ±0.21	0.65 ±0.08
Serotonin	N.D.	N.D.
Sulpiride	N.D.	N.D.

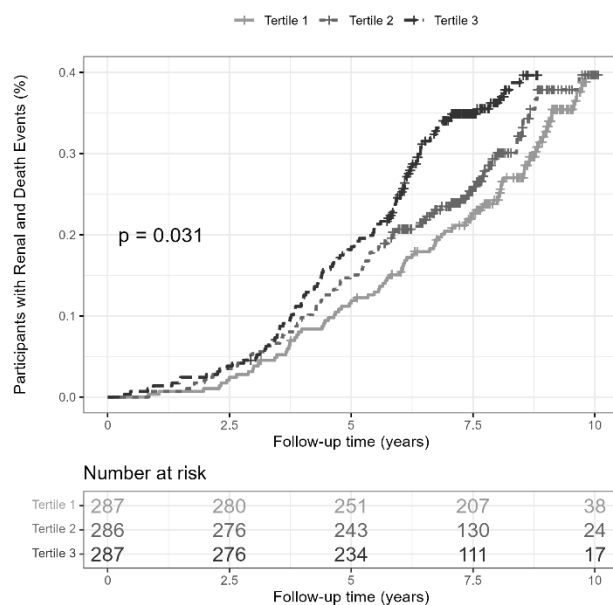
790
791 The metabolites in the kidney were analyzed by ZipChip with LC-MS/MS.
792



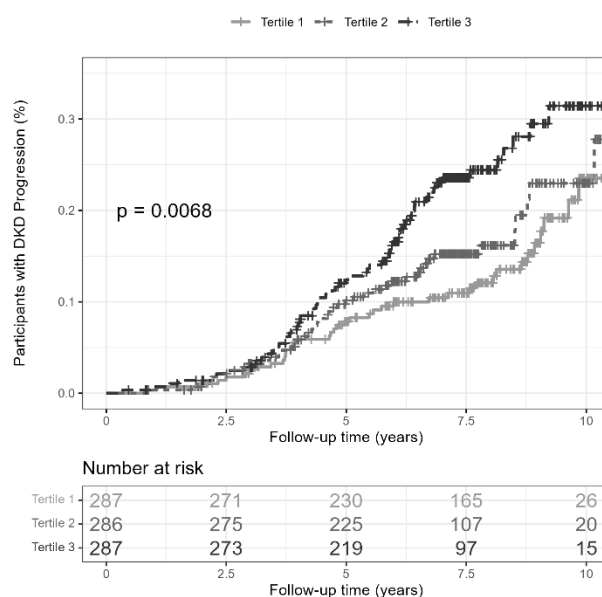
793
794 **Supplementary Figure 1. ZipChip urine adenine/creatinine assay correlates with LC-MS/MS.** A ZipChip urine
795 adenine/creatinine assay was developed and found to highly correlate with urine adenine/creatinine measured by LC-
796 MS/MS. (n=23 samples, $r=0.90$, $p<0.0001$). Raw data was log-transformed and then normalized to urine creatinine.
797 The unit for adenine concentration in the urine is nM/mM creatinine.

798
799
800
801
802
803
804
805
806
807
808
809
810
811
812

813 A.



B.



814

815 **Supplementary Figure 2. High urine adenine/creatinine ratio (UAdCR) levels identify patients with diabetes**
 816 **who are at high risk of ESKD and mortality (A) and ESKD (B) (combined CRIC and SMART2D).** Participants
 817 with diabetes in the CRIC cohort and SMART2D cohorts had UAdCR levels measured within 1 year of enrollment
 818 and followed for 8-10 years. The top tertile had the highest risk of ESKD and all cause mortality (A) and ESKD alone
 819 (B).

820

821

822

823

824

825

826

827

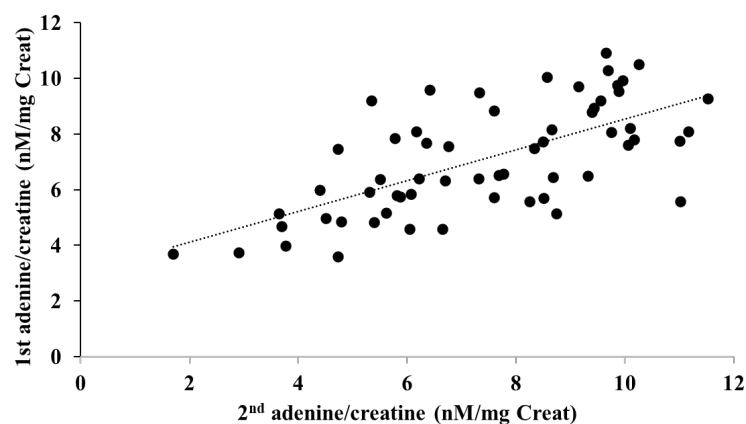
828

829

830

831

832



833

834 **Supplementary Figure 3. Urine adenine/creatinine ratio (UAdCR) levels are stable over time in Pima American**

835 **Indians.** Median time between measures of UAdCR is 12 months (IQR 11.8-12.5 months), $R=0.665$, $p<0.0001$, $n=54$

836 pairs).

837

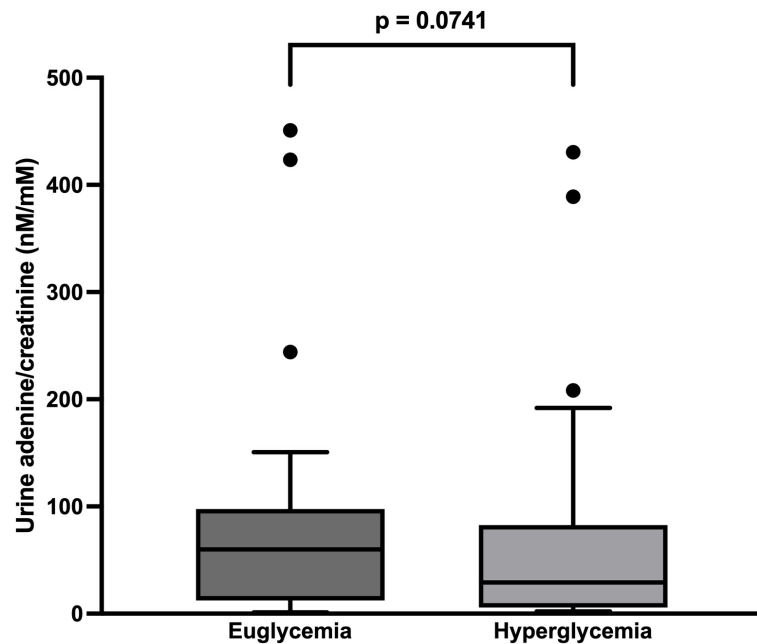
838

839

840

841

842



843

844

845 **Supplementary Figure 4. Hyperglycemia does not increase urine adenine/creatinine ratio (UAdCR) levels.**

846 Patients with T1 diabetes underwent euglycemic clamp or hyperglycemic clamp with UAdCR measured at end of

847 clamp period (n=40 patients) .

848

849

850

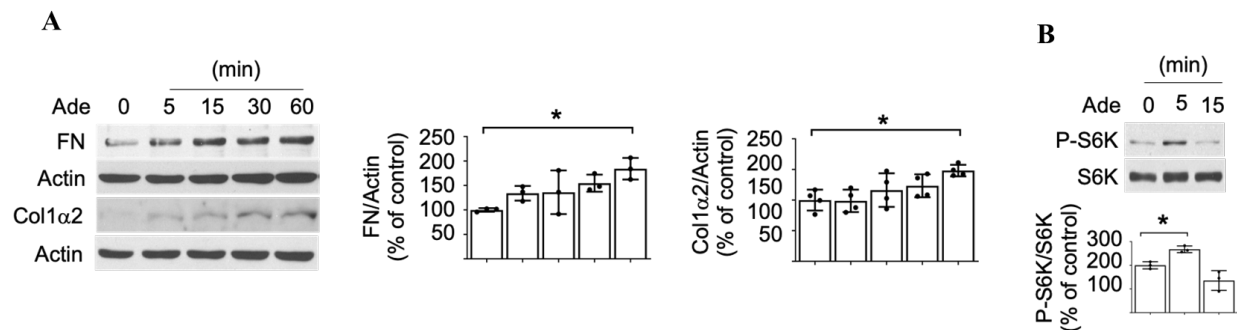
851

852

853

854

855



856

857 **Supplementary Figure 5. Adenine stimulates fibronectin, type I collagen and mTOR in human proximal**

858 **tubular epithelial cells.** Adenine administration to human kidney-2 (HK2) cells increases production of fibronectin

859 and alpha2 chain of type I collagen (A) within 1h. Adenine stimulates mTOR activity within 5m of exposure as

860 measured by phosphorylation of S6 kinase (B) (n=3 samples/group *p<0.05).

861

862

863

864

865

866

867

868

869

870

871

872

873

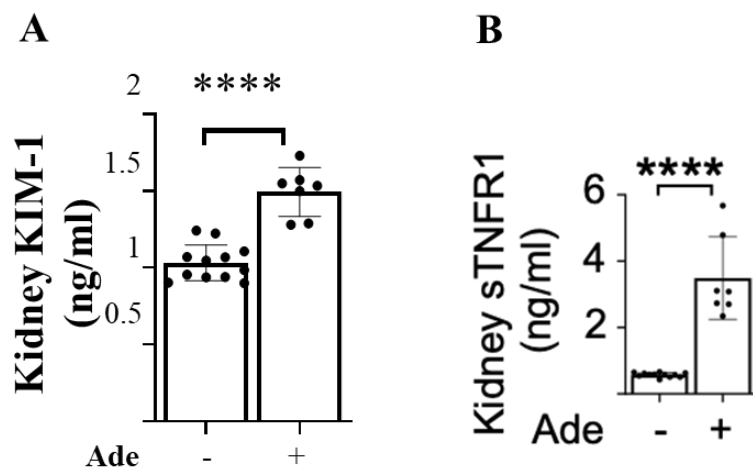
874

875

876

877

878



879

880 **Supplementary Figure 6. Adenine stimulates kidney KIM-1 and kidney sTNFR1 levels.** Adenine administration
881 to mice increases kidney levels of KIM-1 (A) and sTNFR1 (B). (n=12 in control group and n=7 in adenine treated
882 group, ****p<0.001).